# *Enhancing the bearing strength of woven carbon fibre thermoplastic composites through Additive Manufacturing*

***Andrew N. Dickson [1], Denis P. Dowling [1]***

***[1] School of Mechanical & Materials Engineering, University College Dublin, Ireland***

Abstract:

This paper examines a novel additive manufacturing (AM) technique for the fabrication of woven multilaminate composites. The printing studies were carried out using nylon coated carbon fibre Tow in the form of a filament. This pathing technique allows for a woven structure to be integrated with features (such as notches) previously only possible through destructive machining processes. In order to evaluate the performance of these printed composites, bearing response studies were carried out. 6 mm holes were routed into a multilaminate woven composite structure, the resulting part's mechanical performance was then tested and compared with specimens which had been drilled post printing. Specimen were comprised of 9 woven laminates stacked to form a 3.1 mm thick standardised test coupon for single and double shear testing (ASTM D5961). Current industry standard machining techniques result in fibre discontinuity and damage, this results in suboptimal mechanical performance of composite components. These new 'Tailor Woven' specimens achieved single shear bearing strengths of up to 214 MPa and double shear bearing strengths of up to 276 MPa. These values represent an increase of 29% and 63% respectively compared with equivalent composites in which the hole had been drilled.

Keywords: Carbon Fibre, Thermoplastic, Additive Manufacturing, Bearing Response, Continuous Fibre.

# Contents



## 1. Introduction:

*3D printing composites*

The additive manufacturing (AM) of composites is an area of growing interest, with studies on short fibre/particle [1]–[5] and continuous fibre [6]–[17] composites among those reported in recent years. An example of a short fibre study is provided by Ning et al [3], they examined the use of chopped carbon fibre as an additive in an ABS filament, , it was reported to yield an increase in tensile strength and stiffness versus unreinforced equivalents. The content of fibres in these filaments was limited to approximately 10%, as at higher levels the increase in porosity resulted in a reduction in tensile strength, toughness, yield strength and ductility. As a step toward further increased mechanical performance, studies have examined the use of continuous fibre

reinforcement within a polymer printed part. An example of a study of continuous fibre is that of Matsuzaki et al [10], they carried-out studies on a custom in-nozzle impregnation system, this facilitated the printing of Jute or Carbon fibre in a Polylactic acid (PLA) matrix. This study demonstrated a 4-fold increase in tensile strength with the use of carbon fibre over the PLA only specimen. Whilst earlier studies, such as Matsuzaki et al, were typically carried out on custom built printing systems, later studies have focussed on the Markforged line of composite printers. Markforged released the first commercial composite AM system in 2014 utilising continuous carbon, Kevlar and glass fibre in a PA6 (Nylon) matrix. This system has been evaluated by a number of authors [8], [9], [11]–[13].

*Tailored fibre placement / Tape Laying Systems*

Tailored fibre placement (TFP) and fibre steering are techniques for the placement of fibres with the use of sewing or tape systems. Sewing based systems have been utilised in attempts to increase composite performance, and typically follow a path for fibre determined by Finite element models [18]–[20]. These systems utilise an un-sized bundle of mono-filaments, which are fixed to a fabric backing by a thread, guided by a sewing needle. These preformed fibre rows are then placed into a mould, vacuum bagged and impregnated with an appropriate resin. Fibre bundles placed via this method are often unevenly loaded by the fixation threads, this has been reported by Uhlig et al and resulted in changes in volume fraction where threads located [20]. Another method for guiding/placing fibres is that of Tape laying systems. These are typically larger in scale and are used extensively in the aerospace industry for laying of large, relatively flat areas of fibre i.e. aircraft wings [21]. In both technologies mentioned above, unidirectional fibre layers are deposited therefore layers must be deposited at 0 and 90-degree angles to achieve higher mechanical isotropy.

*Woven composite construction*

Woven fibre fabrics constructed on a loom are the most utilised form of reinforcing materials used in small-medium scale applications. These fabrics are typically formed from thousands of fibre tows

threaded together on a loom to form a semi-rigid sheet, this is then cut to size and placed into a mould or forming plate to be impregnated with an appropriate resin or polymer. As the fabrics consist of two or more fibre layers interlocked together, the resulting composites exhibit more isotropic behaviour than obtained for unidirectional composites (mentioned above). As these composite sheets are made to generic sizes, a subsequent machining or water jet cutting processing step is required in order to obtain the required shape and size [22], [23]. As an example, aerospace applications often require machining of composites to facilitate their integration into assemblies of both metal and composite materials (wing boxes, shrouds, nacelles or panelling). Whilst machining ensures more accurate final part dimensions, mechanical machining can result in damage of the reinforcing fibres and/or matrix material [18], this often leads to the use of bulking to increase mechanical performance, increasing weight. A method that has proven successful in limiting fibre damage around a hole to be placed in a composite, is the use of a large heated spike [24], [25]. This spike is driven into the composite laminate and the heating action helps to part the fibre bundles within the matrix. A difficulty however can be the presence of exposed damaged fibres around the hole, as well as fibre path deformation, as the matrix material is burnt off, reducing the potential for load distribution. In this paper the use of additive manufacturing (AM) is investigated as a means of addressing this problem by printing woven multilaminate composites with selective fibre placement for optimisation of internal fibre orientations, particularly around major stress risers such as a notch/hole.

In our previous work the AM technique for producing woven fibre laminates was successfully demonstrated [26]. These structures contained engineered notches where fibres are routed around a region to leave an opening, this results in a continuous fibre structure around the notch. It has been demonstrated that this process retains 93% of the unnotched structures tensile performance. This same process is utilised in this study to produce multilaminate structures through stacking of the aforementioned laminates. In this study, the performance of these AM engineered notched structures is compared with machined equivalents for fastening applications. Through the use of

bearing response testing, the printed structures load bearing capacity in both metal-composite (Double-shear) and composite-composite (Single-shear) bolted joints were assessed.

## 2. Materials & Fabrication Process:

### 2.1. Carbon Fibre & Polymer Filament

Carbon fibre filament was sourced from Markforged CA. These filaments (0.35 mm diameter) consist of two materials, a fibre bundle (reinforcement) and an impregnated polymer (matrix). The fibre bundle consists of approximately 1000, continuous 10 µm diameter monofilaments, this provides the main load bearing component within the filament. The polymer matrix material is a proprietary Nylon blend developed by Markforged. The filament is provided on 150 $cm^3$ spools and stored in a dry box prior to printing, due to Nylons hygroscopic nature.

### 2.2. 3D Printing System

Fibre filament was deposited utilising a Prusa i3 printer chassis with a modified printing head. A 0.6 mm Markforged fibre nozzle was installed. To reduce the heated region and decrease the likelihood of clogging (through fibre snagging), a length of Polytetrafluoroethylene (PTFE) tubing was inserted into the nozzle. For the specimen produced in this study a print temperature of 245°C, and a speed of 10 mm/s was used. The printing was carried out on an unheated Garolite print plate which was coated in a layer of Polyvinyl acetate (PVA), to ensure adequate adhesion during printing.

### 2.3. Fibre Pathing Technique:

As the filaments used in this study contain continuous fibres, it is not possible to stop material feeding after the print has begun (unlike polymer printing). It was therefore necessary to generate a

continuous toolpath (Gcode) with no 'travel' moves. Toolpaths were generated through a parametric Python script, with output commands compiled in a spreadsheet software before transferal to the printer. Outputs generated were customisable by altering of input parameters (such as sample size, weave spacing, feature locations, print speed etc). Note that carbon fibres stiffness precludes the use of tight cornering whilst printing (typically corner radii of <2mm have a higher risk of fibre breakage occurring), it was therefore necessary to take larger sweeping corners to avoid fibre breakages. These cornering paths are shown in Figure 1. Fibre folding occurs at these points as observed by Matsuzaki et al [27], however the toolpath utilised for these samples ensures that these folds are net zeroed by a fold in the opposite direction at the opposite corner of the structure. This ensures that folding does not effect the composites bulk structure.

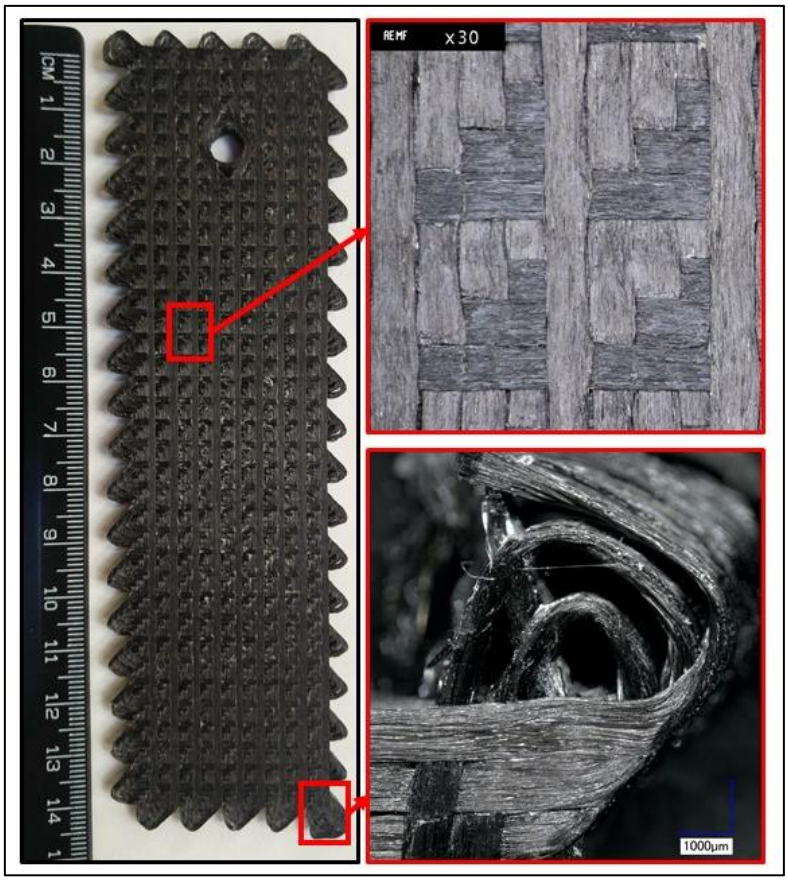


*Figure 1: Woven Carbon Fibre multi-laminate sample with a hole made of steered fibres requiring no post processing. Close-ups of a finished woven layer and cornering structure featuring fibre folding* [27].

The woven structure produced from this technique differs from a standard loomed weave (such as twill, plain or satin) in that a 'flyer' row is always left at the top of the structure. Whilst this would

result in an unstable textile fabric (due to the absence of a binder), in this case the flyer is held in place by the matrix material. A positive side effect of this deposition pattern is the low crimp applied to fibres within the weave, reducing slack between fibre bundle and reducing potential elongation of the laminate before full tension is reached [28]. For all testing in this study the printed composites comprised of 9 layers stacked to form the final 3.1 mm thick test specimen (layer thickness of 0.34-0.35 mm). These layers were stacked automatically by increasing the Z height by the desired height and printing as normal atop the previous layer, in this way, hand layup is not required. Filament lines were placed with a spacing of 0.8 mm, this provides sufficient overlap to form a rigid structure with minimal gaps between lines.

"Tailor Woven" Hole Feature

Previous studies on tailored pathing have utilised a thermally assisted Piercing (TAP) or plug method to divert fibre around a hole into a multi-laminate composite sheet [18], [24], [25], in both cases this leads to resin rich region directly above and below the hole. This resin region allowed bolt travel in the Y-axis as the resin is easily compressed without reinforcement. In this study, fibres from the X and Y axis were diverted around a region to leave a hole with no matrix rich regions, as illustrated in Figure 2. No signs of fibre damage were visible around the notch walls when examined with optical microscopy. In contrast to previous studies utilising TAP or plus techniques, the area around the holes contains a higher fibre content than that of the bulk structure. This region could therefore potentially act as a 'buffer-zone' for mitigating damage associated with movement of a fastener inserted in the hole. The as printed hole diameter was 6.1± 0.07 mm. This diameter was achieved through the use of a Gcode set diameter of 8.3 mm, results for set versus actual hole diameter were similar to those observed by Matsuzaki et al [27], and is the result of fibre bundles 'folding back' as the outer fibres are travelling along a longer path than that of the inner fibres. It was demonstrated that in radii greater than 10 mm this effect is mitigated. This steering mechanism, in addition to the overlapping of fibre paths, leads to a local increase in layer height. Layer heights in this area are typically 10% higher than the bulk structure, in this test case the thickness of the laminate around

the hole was on average 3.4 mm thick. This will be diminished in future through staggering of hole diameter to spread fibre bundles more evenly around the region. The extent of fibre bundle compression and air void content around the hole have been characterised in a previous study [26], with air contents found to be as low as 1% in this region.

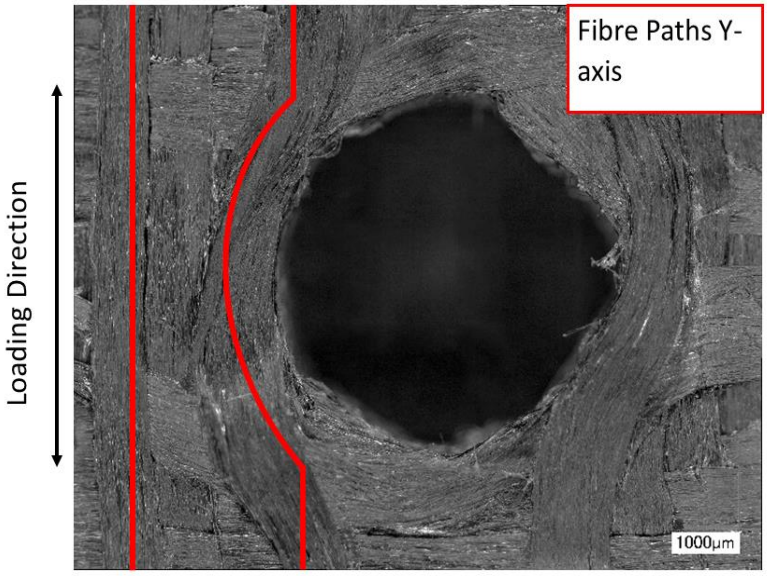


*Figure 2: Fibre pathing in the Y-axis around the Hole feature and fibre path in straight woven sections (red lines indicate fibre path and displacement associated with curving around the hole).*

## 3. Experimental Setup:

### 3.1. Specimen Preparation

ASTM D5961 Bearing response testing was utilised to assess the AM multi-laminate structures response to bolted fastening. Both Single-Shear (Procedure B) and Double-shear testing (Procedure A) was employed from this standard, with 'Tailor woven' holes and 'Drilled' holes bearing strengths compared.

'Drilled' test specimens were evaluated as a comparison with the 'Tailor woven' composites. The latter were obtained by drilling the composite using a diamond coated drill-bit to a target diameter that would fit tightly around an M6 bolt with minimum clearance. A series of holes were drilled with rotational-speeds ranging from 1200 – 7500 RPM, and feedrates from 11 – 86 cm/min (outside of these ranges the composite was either not penetrated, or excessive damage was caused for

consideration). Final feed and speed rates were set at 53 cm/min and 7500 RPM. These parameters where determined by examining literature values for drilling of epoxy matrix materials, these were used as a starting point for testing and settings were changes based on results obtained. The nylon matrix used is extremely tough and is more tolerant to high speed drilling than epoxy based composites [21–25]. This process was utilised to minimise fibre damage around the hole circumference. A final hole diameter of 5.9±0.04 mm was achieved with minimal delamination or fibre displacement (See Figure 3).

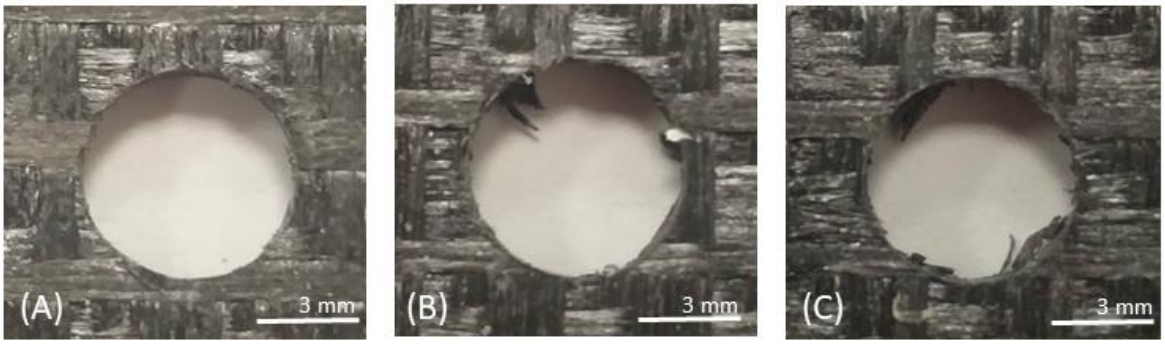


*Figure 3: Optimised drilling parameters (Tool rotational speed, tool feed-rate), (A) achieved the cleanest cut and had no visible surface damage or delamination present, this was then used for following tests :(A) 7500 RPM, 53 cm/min; (B) 2800 RPM, 53 cm/min (C)1600 RPM, 53 cm/min.*

Test specimens had dimensions of 140 x 36 x 3.1 mm (excluding selvedge regions) with a centred 6 mm hole placed 18mm from the leading edge of the sheet. 'Tailor Woven' specimen were created by guiding fibres around the hole and required no post processing before testing (as described in section 2.3.). As cutting of selvedge 'tabs' may have introduced new variable to testing, the tabs were left in place.

### 3.2. Specimen Porosity

Micro-Computed Tomography (µCT)

Printed specimen were inspected under Micro-CT using a GE Phonenix Nanotom M system in order to establish the level of porosity (air void content) within the printed structure. Excessive porosity may reduce fibre-matrix contact and result in poorer load transfer between adjacent fibres through

matrix material. It is therefore important to assess the occurrence (if any) of air void infiltration within composite material.

Samples for CT were sectioned to a size of 40 x 13 mm from a 50 x 50 mm plate printed using the same layup steps as the bearing specimen and mounted into a polystyrene mount. This ensures that the entire sample can be imaged, as the density of the mount is significantly lower than that of the composite, it can be filtered out of the final images. Scans were performed at a Voltage of 70 Kv and current of 120 µA. Following scanning image data was analysed using the VGStudio Max 3.2 analysis tool. By separating air content from solid content via a thresholding-based method, it was possible to calculate the percentage volume of air within the samples. 5 samples were examined using this method, an example of 1 sample is shown in Figure 4. As the volume of each section examined varied from sample to sample a weighted average was utilised, thus providing a more accurate representation of the bulk materials air content. Average porosity is shown in Table 1.

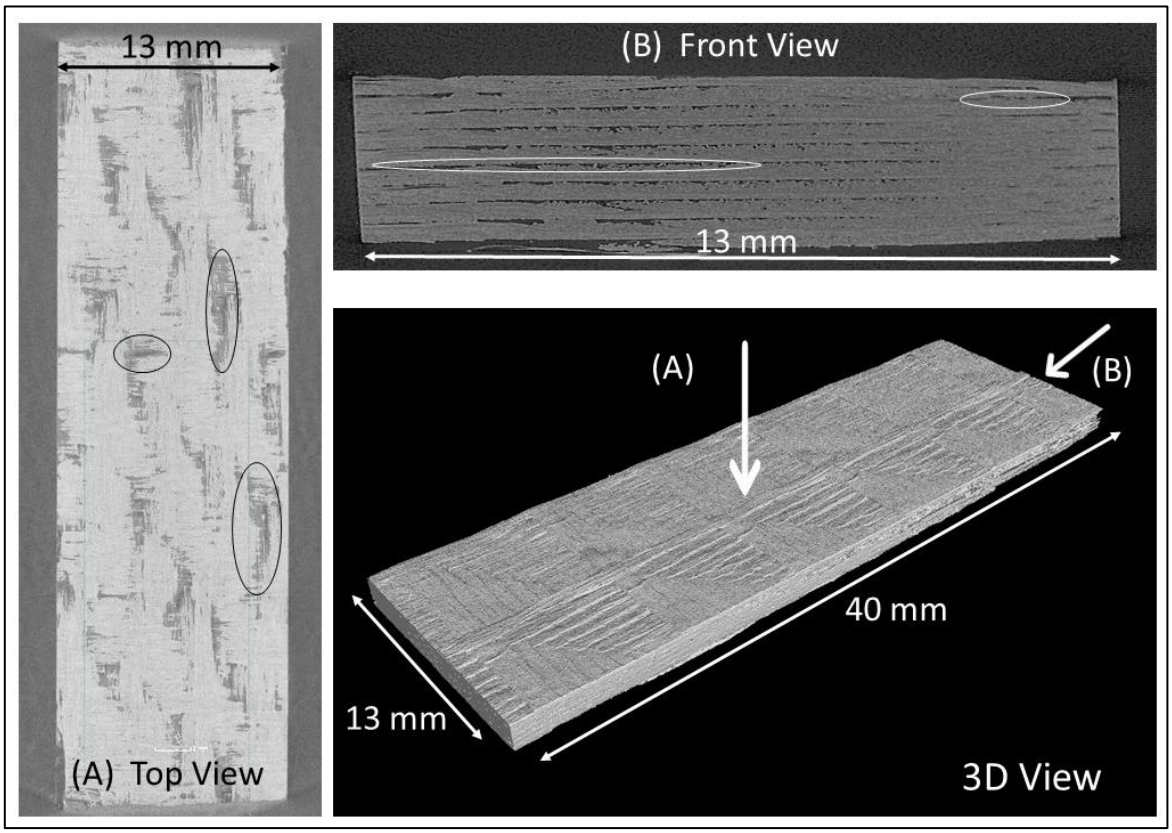


*Figure 4: µCT scans illustrate the porosity within the samples. Voids are circled as examples. (A) Top view of the sample at the midpoint of the sample thickness, voids are observed at points of fibre overlap. (B) Front view of the sample showing significant void formation along interlaminar planes.*

*Table 1: Average composite porosity as percentage of total volume*

| | Void Volume % |
|---|---|
| Average | 12.80 |
| St Dev | 3.76 |

As is evident from the CT imaging of Figure 4, the major sources of void formation are the interlaminar boundary and the points of contact between the Weft and Warp fibre tows. Interlaminar voids are attributed to excessively rapid cooling of the nylon matrix sufficient to reduce matrix-matrix contact during the melt phase.

### 3.3. Mechanical Testing

Bearing response tests were performed utilising an Instron 100 KN 8501 hydraulic tester. As per the ASTM D5961 (Bearing response) standard the specimens were held in place using Hydraulic clamps and tested at a crosshead speed of 2 mm/minute. Hydraulic grips were used to ensure equal gripping pressure on each tab (500 PSI). A preload of 5 N was applied to each specimen prior to test start to take up slack from gripping apparatus.

#### ASTM D5961 Procedure A – Double Shear

For this test the specimens were held in a steel support structure using a steel M6 nut and bolt, tightened to a torque of 3 Nm (using a Torqueleader ADS 4, 0.8 – 4 Nm, torque wrench). This structure evenly applies shear from either side of the specimen to pull the fastener vertically in a tensile test. This procedure is suggested as a characterisation of the base material/structure for comparison purposes [34]. Five samples of each specimen type were tested.

#### ASTM D5961 Procedure B - Single Shear

Carbon Epoxy Doublers were adhesively bonded to the gripping ends of each specimen to ensure proper alignment. A steel M6 nut and bolt were then used to fasten the two specimen together with an applied torque of 3Nm. Two M6 washers acted as pressure distributors on either side. This single

shear test is typically useful for evaluation of a specific joint configuration [34]. Ten samples of each specimen type were tested (2 per test).

### 3.4. Digital Image Correlation (DIC)

This system was used as a video extensometer for all testing to ensure accurate extension measurement. For this detection system to function, a random pattern must be present on the samples surface. A white coloured elastic spray paint was used to speckle the surface with this pattern. As per Standard ASTM D5961 virtual extensometers are placed on either side of the composite, adjacent to the fastener location, the average of which corrects for any in-plane rotation. As the DIC system is a non-contact measurement there is no inertia lag or risk of surface damage to the specimen under testing.

## 4. Results & Analysis:

### 4.1. Bearing Response Testing (ASTM D5961): A and B

As detailed in the previous section the mechanical performance of the composites was assessed using both single and double shear bearing response. This was in order to evaluate the structures response to in-hole applied loads, typically experienced in fastened composite assemblies. The ASTM standard involves the use of two test methods, firstly to assess the materials structure in

response to fastening (A), and secondly to assess a specific composite-composite fastener joint configuration (B). Test configurations are shown schematically in Figure 5.

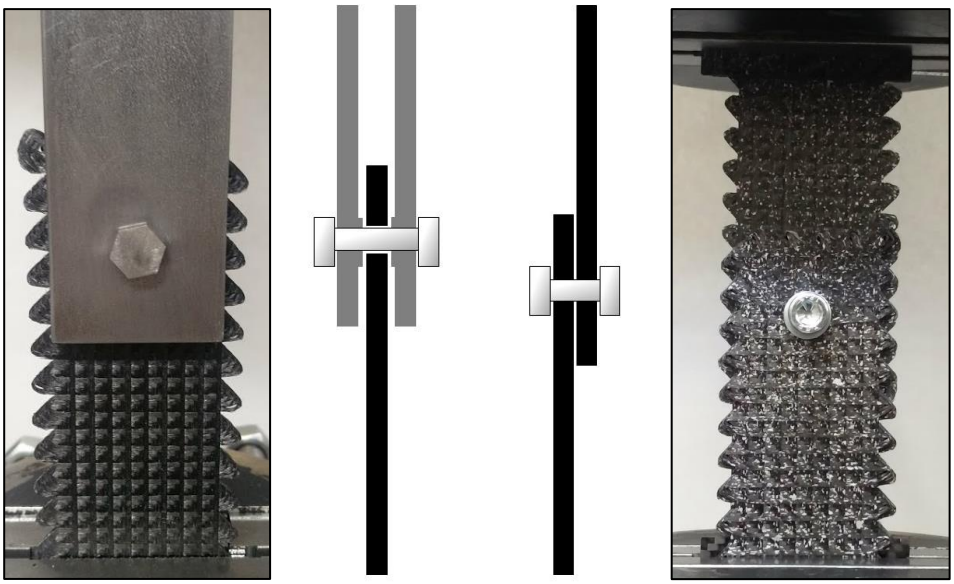

*Figure 5: Procedure A: Double Shear (left) and Procedure B: Single Shear (right) setups prior to testing, also included are diagrams of setup showing fastener positions.*

Calculations of Bearing strain and Bearing Strain were performed in line with ASTM D5961 utilising the Equations 1 & 2 respectively.

$$F^{bru} = \frac{P^{max}}{(k * D * h)} \qquad \textit{Equation 1}$$

$F^{bru} = Ultimate\ Bearing\ Strength, MPa,$

$P^{max} = Maximum\ Load\ prior\ to\ failure, N,$

$D = Hole\ Diameter, \quad h = thickness\ of\ specimen, \quad k = Load\ per\ hole\ (1\ for\ single\ fastener\ test)$

$$\in_i^{br} = \frac{(\delta_{1i} + \delta_{2i})/2}{K * D} \qquad \textit{Equation 2}$$

$\epsilon_i^{br} = Bearing\ Strain, Microstrain$

$\delta_{1i} = extensometer\ 1\ displacement, \delta_{2i} = extensometer\ 2\ displacement$

$K = 1.0\ for\ double\ shear, 2.0\ for\ single\ shear$

4.1.1. Procedure A (Double Shear):

Double shear testing demonstrated that the 'Tailor Woven' specimens outperformed the 'Drilled' specimens by 63 % with Bearing strengths of up to 276 MPa and 169 MPa respectively (Figure 6). Tailor woven samples exhibited significantly decreased notch deformation and a bearing strain of just 55% of that obtained for the drilled specimens (Figure 7). The Tailor Woven specimens did however experience a sharper 'kink' zone at strain 0.02-0.03 possibly resulting from slightly higher bolt-hole clearance. Future work will aim to increase hole diameter consistency across the thickness of the laminate.

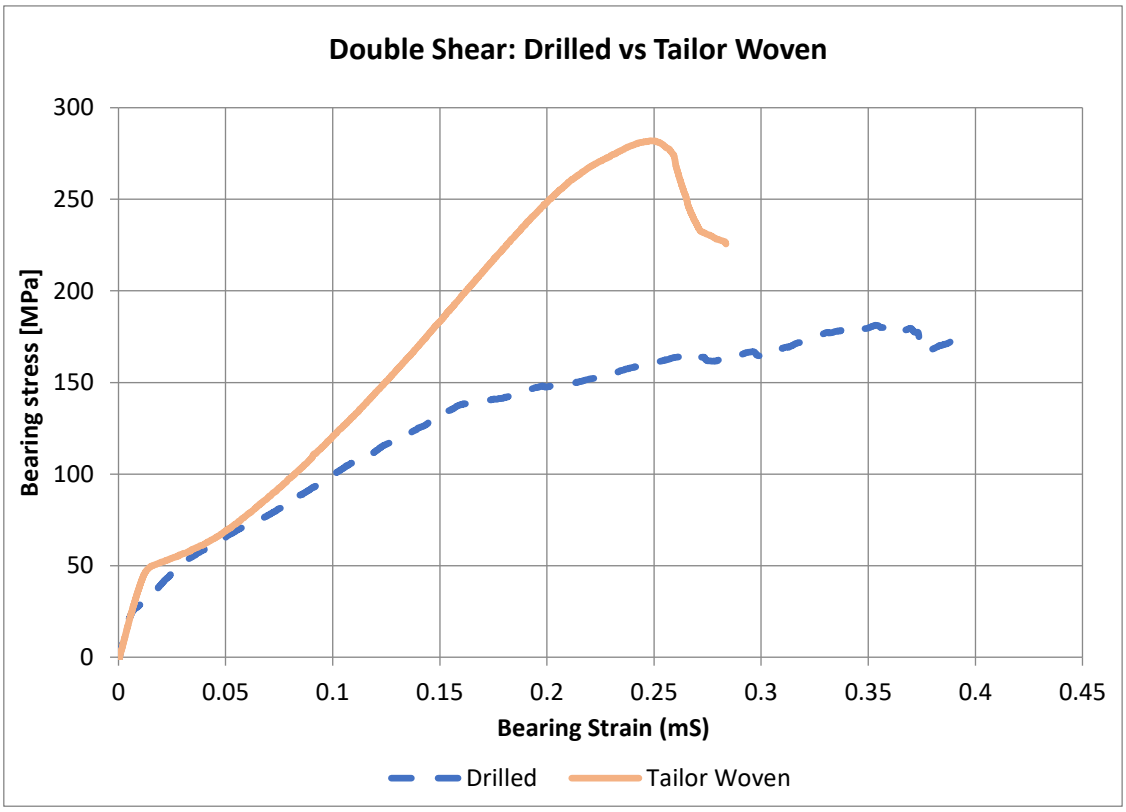


*Figure 6: Example Bearing Stress/ Bearing Strain curves for double shear test specimen.*

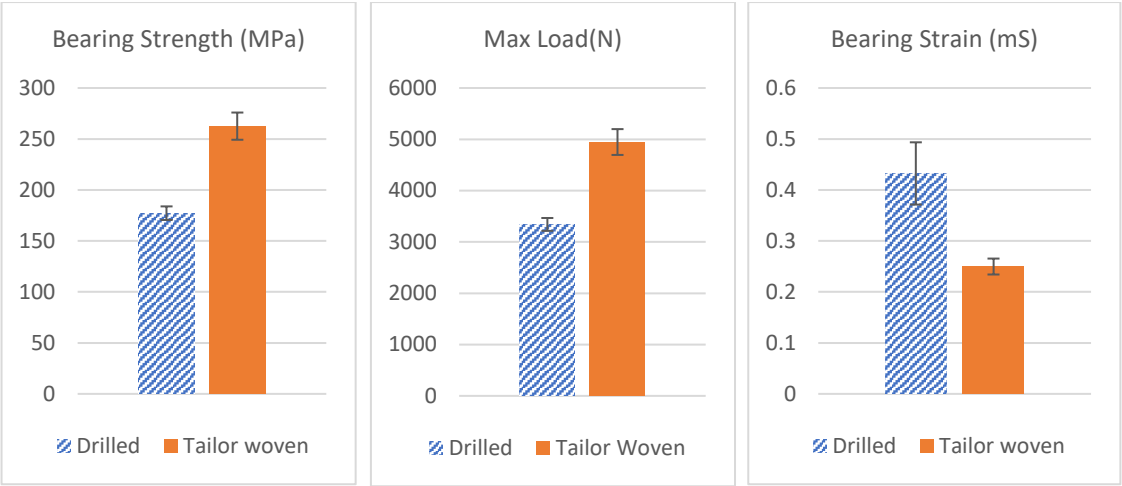


*Figure 7: Averaged test results for Bearing Strength, Maximum load and Bearing Strain for double shear testing*

### 4.1.2. Double Shear Damage Analysis

Cross-sectional analysis was performed to identify internal damage to the tested composites. Specimens were cut along their length through the midsection of the hole, and then mounted in acrylic resin. Wet sanding was then used to ensure a smooth finish for observation. Optical microscopy was used for close examination of the specimens. Double shear failure mode was consistent with type B1I failure in all cases, this is the only acceptable form of failure according to the standard ASTM D5961 (Figure 8). Bearing failure is characterised by fastener travel through the bulk of the laminate in the direction of testing, this is often observed in the form of surface buckling. Net tension or cleavage failure both entail sections of the composite detaching from the bulk due to crack propagation and are not valid failure modes for this test.

In the case of the drilled specimens it was found to be difficult in identifying a clear maximum force peak, a failure threshold of 5% Max Load was therefore used to identify when a maximum force has clearly been reached [34]. The Tailor Woven specimen exhibited a distinct peak in load before dropping sharply, facilitating endpoint determination. Rapid test termination after a maximum force has been reached is essential so as to prevent masking of the true failure mode by large-scale hole distortion [34].

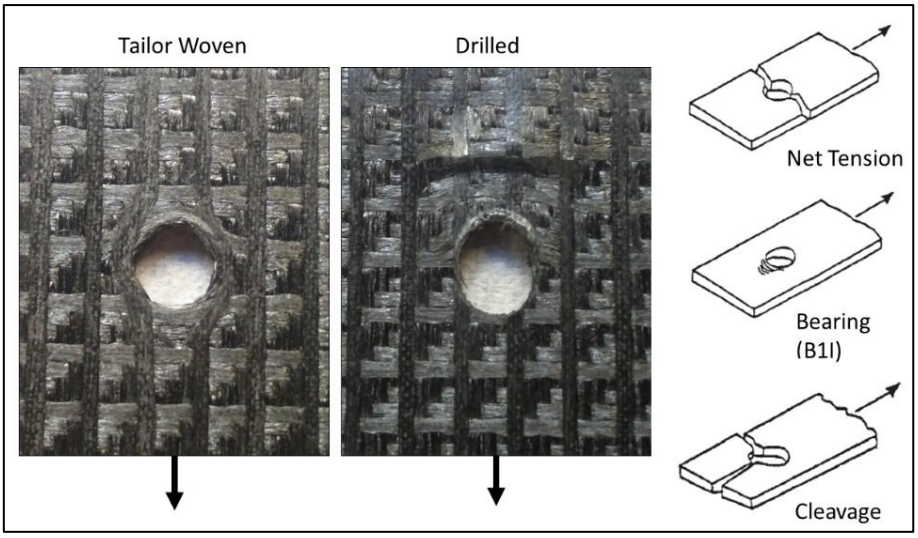


*Figure 8: Specimen with bolt removed after testing. Examples of typical failure modes are displayed (right) of which bearing failure is the only acceptable type for determining the composites response*[34].

Analysis of drilled specimens using optical microscopy revealed two major modes of failure, these being compression failure above the hole location and tensile failure on the flanking sides of the hole, as seen in Figure 9. Major buckling is seen in drilled specimens above the hole, this being the result of compression of the discontinued fibres. In contrast, Tailor Woven specimens exhibit reduced damage with the majority of damage as a direct result of tensile loading, in which fibre composites typically excel. Upon closer inspection minor compressive damage has occurred above the hole location (Figure 9). Some fibre displacement is also visible on the top side of the hole where the bolt has elongated the hole, this elongation is however minor compared to that observed in the case of the drilled specimen. The extent of this damage is significantly reduced in the case of the Tailor Woven specimens, demonstrating the increased mechanical strength of the printed hole structure.

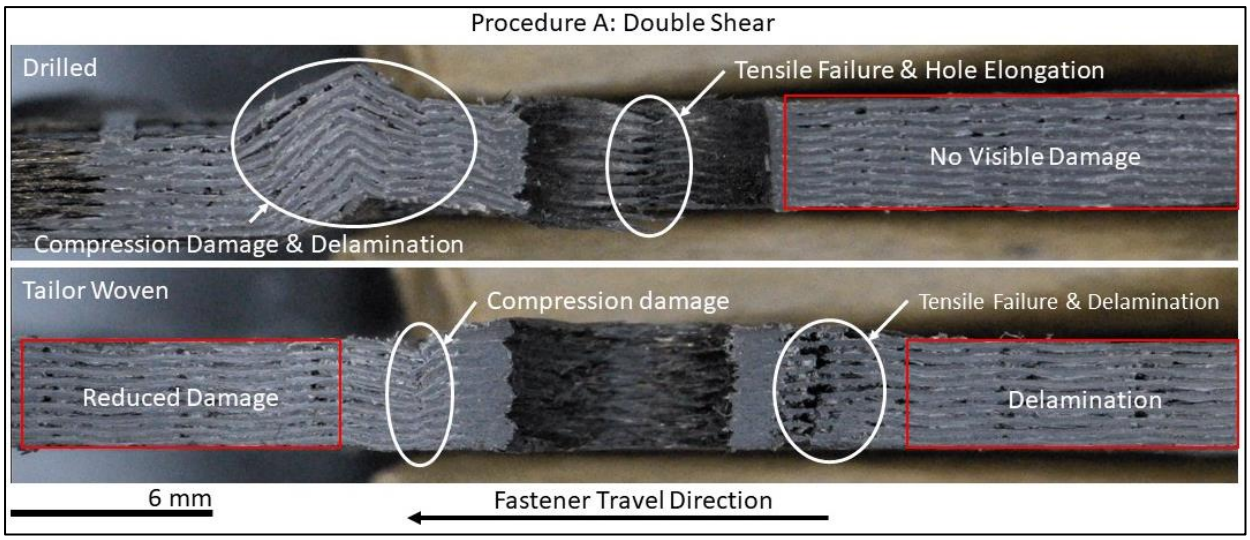


*Figure 9: Double shear failure regions for Drilled (Top) and Tailor Woven (Bottom) specimen. Both Compressive and Tensile damage are observed in failed specimen. The location of the tensile failure outside the hole area in Tailor Woven samples has resulted in decreased hole distortion.*

#### 4.1.3. Procedure B (Single Shear):

Single shear testing demonstrated that 'Tailor Woven' outperformed 'Drilled' by 29 % with Bearing strengths of up to 214 MPa and 166 MPa respectively (Figure 10Figure 11).

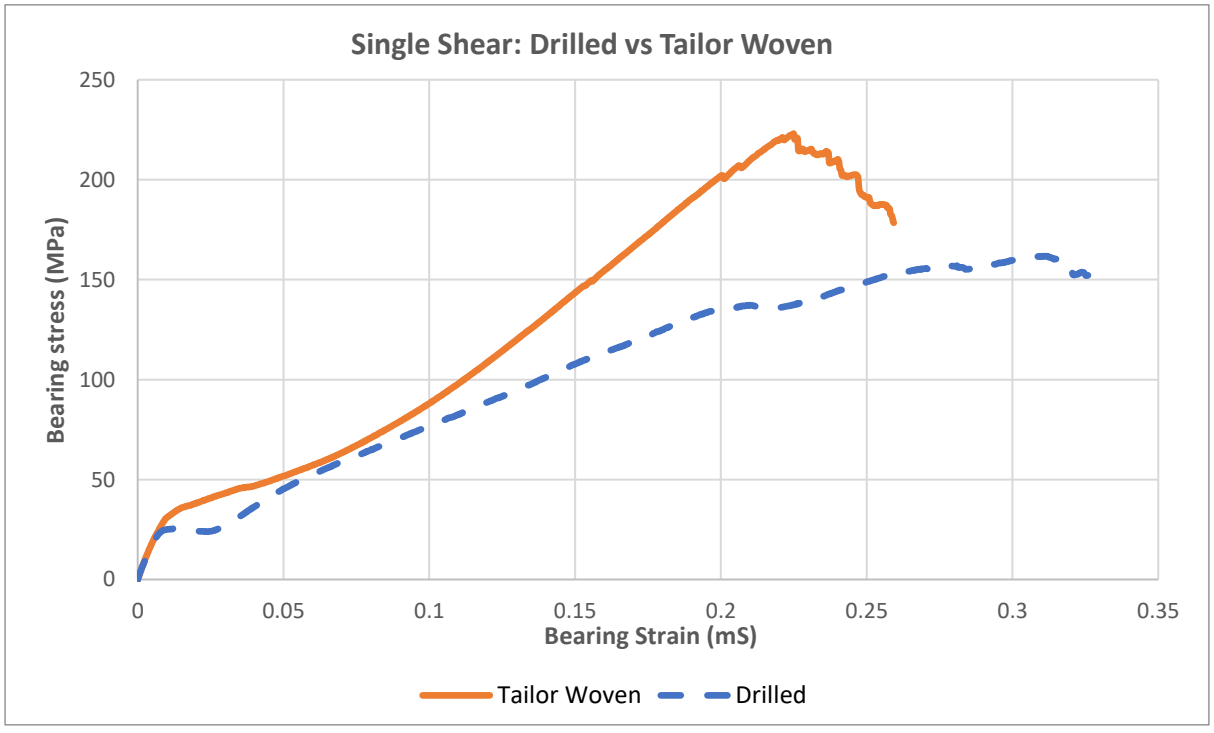


*Figure 10: Example Bearing Stress/Bearing Strain Curve for a single shear test specimen.*

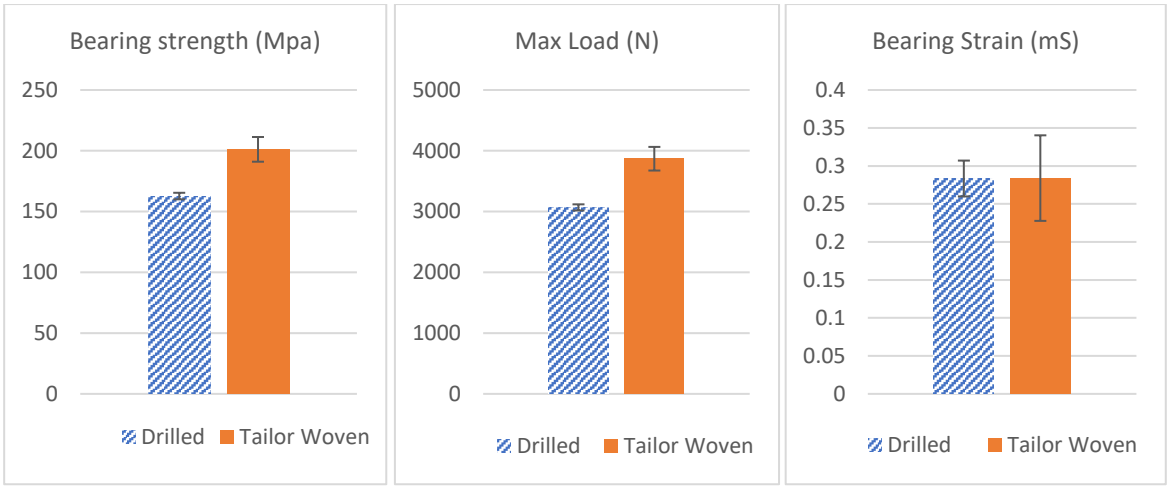


*Figure 11: Averaged test results for Bearing Strength, Maximum Load, and Bearing Strain for single shear testing*

### 4.1.4. Single Shear Damage Analysis

Cross sectional analysis was performed using the process highlighted in 4.1.2. to determine the extent of internal damage to the composite. Procedure B specimen also exhibited bearing failure in accordance with code B1I (Figure 12).

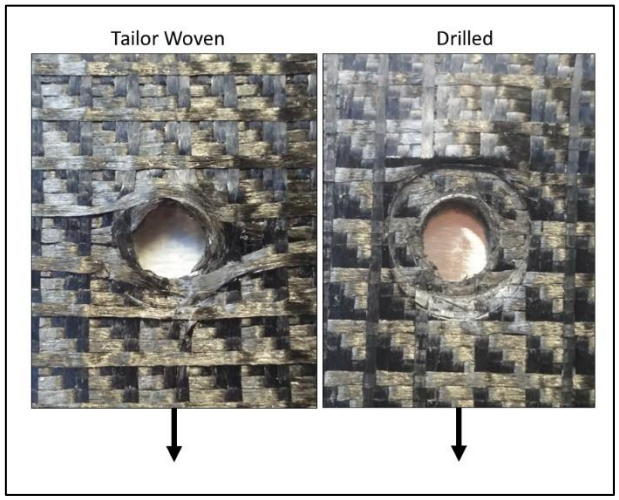


*Figure 12: The tailor woven and drilled specimen with bolt removed after testing.*

Matrix and fibre damage around the washer contact region are as a result of the bolt rotating under shear, forcing the washer into the laminate cutting fibres and weakening the surrounding structure. As demonstrated in Figure 12 the Tailor Woven specimen exhibited superior resistance against the compressive load caused by bolt rotation, thereby reducing the movement of the bolt. The densified

region around the hole acted as a buffer zone preventing compression and distributing load into the surrounding area. Buckling resulting from compressive loading is observed above the hole in the case of the drilled specimens (Figure 13). The continuous fibres also allowed the bolt to be held with fibre in tension rather than compression (in the case of drilled specimen), in which the high strength fibres excel. This would also explain the occurrence of delamination in both specimen types. As compression was the main load experienced in drilled specimen, delamination occurs above the hole due to buckling. For the Tailor Woven specimens delamination is observed below the hole as the laminates are pulled into tension, the woven fibres are straightened and cause disbonds to occur at weave intersection points.

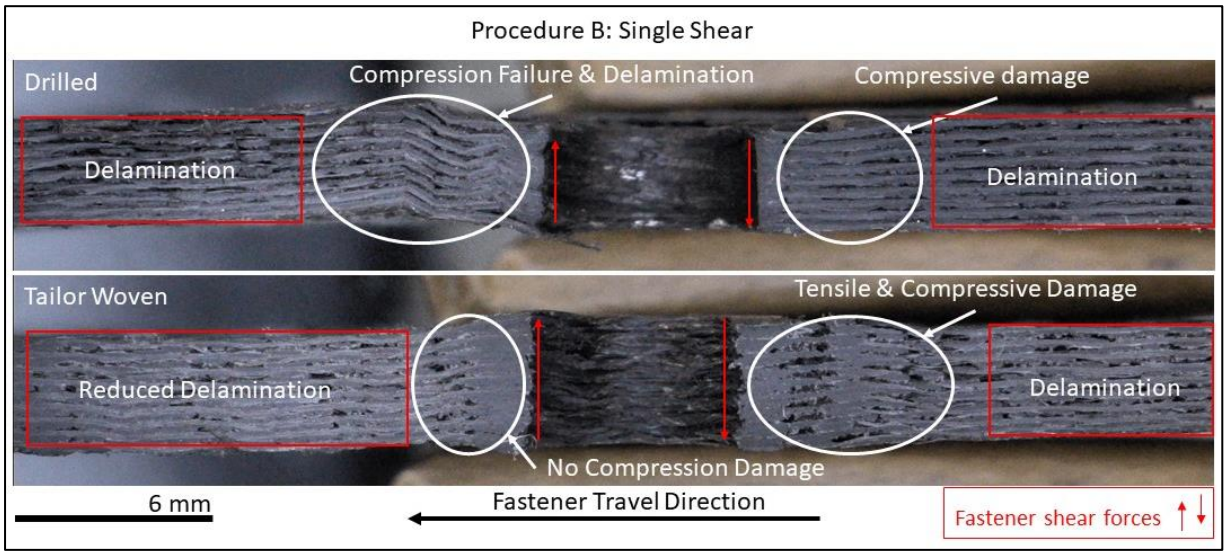


*Figure 13: Single Shear failure regions for Tailor Woven and Drilled specimen. Damage in Tailor Woven specimen is primarily the result of tensile forces versus major compressive damage observed in Drilled specimen.*

## 5. Conclusions

Through an additive manufacturing technique, woven multilaminate carbon fibre reinforced composite structures have been produced for the first time. This printing technique has demonstrated its ability to auto layup woven multilaminate structures containing apertures/holes without the need for post-machining. These fibre structures were continuous in nature, with no break in fibre continuity around the hole perimeter. When tested according to the approach

detailed in ASTM D5961 which is the industry standard for fastening performance, the multilaminate structures for fastening applications exhibited bearing strengths up to 63% higher in double, and 29% higher in single shear than the equivalent drilled/machined specimen representing the current industry standard for fastening performance. Significantly reduced fibre damage and fastener travel were characteristic of the new process versus benchmark drilled specimens. This fibre placement technique has potential application in aerospace and automotive industries for increasing fastened composite assembly strengths and stiffness versus drilled techniques. This enhanced bearing strength can be achieved without additional bulking of joints, reducing assembly weights.

## 6. Acknowledgements

Supported by Irish Manufacturing Research and by SFI through the I-Form Advanced Manufacturing Research Centre 16/RC/3872.

Funding for procurement of the X-Ray µCT scanner was provided through a Science Foundation Ireland infrastructure award (16/RI/3747) and is directed by Dr. Saoirse Tracy.

## 7. Data Availability

The raw/processed data required to reproduce these findings cannot be shared at this time due to legal and technical reasons.

## 8. References

[1] H. L. Tekinalp, V. Kunc, G. M. Velez-Garcia, C. E. Duty, L. J. Love, A. K. Naskar, C. A. Blue, and S. Ozcan, “Highly oriented carbon fiber-polymer composites via additive manufacturing,” *Compos. Sci. Technol.*, vol. 105, pp. 144–150, 2014.

[2] W. Zhong, F. Li, Z. Zhang, L. Song, and Z. Li, “Short fiber reinforced composites for fused deposition modeling,” *Mater. Sci. Eng. A*, vol. 301, no. 2, pp. 125–130, 2001.

[3] F. Ning, W. Cong, J. Qiu, J. Wei, and S. Wang, “Additive manufacturing of carbon fiber

reinforced thermoplastic composites using fused deposition modeling," *Compos. Part B Eng.*, vol. 80, pp. 369–378, 2015.

[4] D. Bue, J. Skov, T. Hofstaetter, D. B. Pedersen, J. S. Nielsen, M. Mischkot, and H. N. Hansen, "Investigation of digital light processing using fibre-reinforced polymers."

[5] Stepashkin, D. I. Chukov, F. S. Senatov, A. I. Salimon, A. M. Korsunsky, and S. D. Kaloshkin, "3D-printed PEEK-carbon fiber (CF) composites: Structure and thermal properties," *Compos. Sci. Technol.*, vol. 164, pp. 319–326, Aug. 2018.

[6] X. Tian, T. Liu, Q. Wang, A. Dilmurat, D. Li, and G. Ziegmann, "Recycling and remanufacturing of 3D printed continuous carbon fiber reinforced PLA composites," *J. Clean. Prod.*, vol. 142, pp. 1609–1618, 2017.

[7] M. Namiki, M. Ueda, A. Todoroki, Y. Hirano, and R. Matsuzaki, "3D Printing of Continuous Fiber Reinforced," *Proc. Soc. Adv. Mater. Process Eng. 2014, Seattle, 2-5 June 2014, 6*, pp. 2–7, 2014.

[8] G. D. Goh, V. Dikshit, A. P. Nagalingam, G. L. Goh, S. Agarwala, S. L. Sing, J. Wei, and W. Y. Yeong, "Characterization of mechanical properties and fracture mode of additively manufactured carbon fiber and glass fiber reinforced thermoplastics," *Mater. Des.*, vol. 137, pp. 79–89, Jan. 2018.

[9] J. Justo, L. Távara, L. García-Guzmán, and F. París, "Characterization of 3D printed long fibre reinforced composites," *Compos. Struct.*, vol. 185, pp. 537–548, Feb. 2018.

[10] R. Matsuzaki, M. Ueda, M. Namiki, T.-K. Jeong, H. Asahara, K. Horiguchi, T. Nakamura, A. Todoroki, and Y. Hirano, "Three-dimensional printing of continuous-fiber composites by in-nozzle impregnation.," *Sci. Rep.*, vol. 6, p. 23058, Mar. 2016.

[11] F. Van Der Klift, Y. Koga, A. Todoroki, M. Ueda, Y. Hirano, F. Van Der Klift, Y. Koga, A. Todoroki, M. Ueda, Y. Hirano, and R. Matsuzaki, "3D Printing of Continuous Carbon Fibre Reinforced Thermo-Plastic ( CFRTP ) Tensile Test Specimens," *Open J. Compos. Mater.*, vol. 6, no. January, pp. 18–27, 2016.

[12] V. Dikshit, Y. L. Yap, G. D. Goh, H. Yang, J. C. Lim, X. Qi, W. Y. Yeong, and J. Wei, "Investigation of out of plane compressive strength of 3D printed sandwich composites," *IOP Conf. Ser. Mater. Sci. Eng.*, vol. 139, p. 012017, 2016.

[13] A. N. Dickson, J. N. Barry, K. A. McDonnell, and D. P. Dowling, "Fabrication of continuous carbon, glass and Kevlar fibre reinforced polymer composites using additive manufacturing,"

*Addit. Manuf.*, vol. 16, pp. 146–152, 2017.

[14] H. Al Abadi, H.-T. Thai, V. Paton-Cole, and V. I. Patel, "Elastic properties of 3D printed fibre-reinforced structures," *Compos. Struct.*, vol. 193, pp. 8–18, Jun. 2018.

[15] H. Brooks, D. Tyas, and S. Molony, "Tensile and fatigue failure of 3D printed parts with continuous fibre reinforcement," *Int. J. Rapid Manuf.*, vol. 6, no. 2/3, p. 97, 2017.

[16] M. A. Caminero, J. M. Chacón, I. García-Moreno, and J. M. Reverte, "Interlaminar bonding performance of 3D printed continuous fibre reinforced thermoplastic composites using fused deposition modelling," *Polym. Test.*, vol. 68, pp. 415–423, Jul. 2018.

[17] K. Sugiyama, R. Matsuzaki, M. Ueda, A. Todoroki, and Y. Hirano, "3D printing of composite sandwich structures using continuous carbon fiber and fiber tension," *Compos. Part A Appl. Sci. Manuf.*, vol. 113, pp. 114–121, Oct. 2018.

[18] E. G. Koricho, A. Khomenko, T. Fristedt, and M. Haq, "Innovative tailored fiber placement technique for enhanced damage resistance in notched composite laminate," *Compos. Struct.*, vol. 120, no. November 2015, pp. 378–385, 2015.

[19] P. J. Crothersbf, K. Drechsler ', D. Feltinc, I. Herszberga, and T. Kruckenbergd, "Tailored fibre placement to minimise stress concentrations," *Compos. Part A*, vol. 28, no. 6, pp. 19–625, 1997.

[20] K. Uhlig, M. Tosch, L. Bittrich, A. Leipprand, S. Dey, A. Spickenheuer, and G. Heinrich, "Meso-scaled finite element analysis of fiber reinforced plastics made by Tailored Fiber Placement," 2016.

[21] D. H. J. A. Lukaszewicz, C. Ward, and K. D. Potter, "The engineering aspects of automated prepreg layup: History, present and future," *Compos. Part B Eng.*, vol. 43, no. 3, pp. 997–1009, 2012.

[22] Y. Harada, K. Kawai, T. Suzuki, and T. Teramoto, "Evaluation of Cutting Process on the Tensile and Fatigue Strength of CFRP Composites," *Mater. Sci. Forum*, vol. 706–709, pp. 649–654, Jan. 2012.

[23] C. Santiuste, A. Olmedo, X. Soldani, and H. Migué Lez, "Delamination prediction in orthogonal machining of carbon long fiber-reinforced polymer composites."

[24] W. Hufenbach, R. Gottwald, and R. Kupfer, "Bolted Joints with moulded holes for textile thermoplastic composites," *Technology*, pp. 1–6, 2011.

[25] C. M. W. N.W.A. Browna,b, S.L. Oginb, and and P.A. Smithb, “Investigation into the mechanical properties of thermoplastic composites containing holes machined by a thermally-assisted piercing (TAP) process,” 2017.

[26] A. N. Dickson, K.-A. Ross, and D. P. Dowling, “Additive Manufacturing of Woven Carbon Fibre Polymer Composites,” *Compos. Struct.*, vol. 206, pp. 637–643, Dec. 2018.

[27] R. Matsuzaki, T. Nakamura, K. Sugiyama, M. Ueda, A. Todoroki, Y. Hirano, and Y. Yamagata, “Effects of Set Curvature and Fiber Bundle Size on the Printed Radius of Curvature by a Continuous Carbon Fiber Composite 3D Printer,” *Addit. Manuf.*, vol. 24, pp. 93–102, Dec. 2018.

[28] D. P. C. Aiman, M. F. Yahya, and J. Salleh, “Impact properties of 2D and 3D woven composites : A review,” in *AIP Conference Proceedings AIP Conference Proceedings Journal of Applied Physics*, 2016, vol. 17741, no. 10, p. 020002.

[29] M. K. Nor Khairusshima, A. K. N. Aqella, and I. S. S. Sharifah, “ScienceDirect Optimization of Milling Carbon Fibre Reinforced Plastic using RSM,” *Procedia Eng.*, vol. 184, no. 184, pp. 518–528, 2017.

[30] R. Teti, “Machining of Composite Materials,” *CIRP Ann.*, vol. 51, no. 2, pp. 611–634, Jan. 2002.

[31] P. C. Priarone, M. Robiglio, R. Melentiev, and L. Settineri, “ScienceDirect Diamond drilling of Carbon Fiber Reinforced Polymers: Influence of tool grit size and process parameters on workpiece delamination,” *Procedia CIRP*, vol. 66, pp. 181–186, 2017.

[32] P. Kavan, “Pigment & Resin Technology Investigation and optimization of machining parameters in drilling of carbon fiber reinforced polymer (CFRP) composites Investigation and optimization of machining parameters in drilling of carbon fiber reinforced polymer (CFRP) composites,” *Pigment Resin Technol.*, vol. 46, no. 1, 1108.

[33] M. Harris, M. Asif, M. Qureshi, M. Q. Saleem, S. A. Khan, M. Mahmood, and A. Bhutta, “Carbon fiber-reinforced polymer composite drilling via aluminum chromium nitride-coated tools: Hole quality and tool wear assessment.”

[34] C. Materials and S. Precision, “Standard Test Method for Bearing Response of Polymer Matrix Composite Laminates 1,” vol. i, pp. 1–33, 2014.